A&A 442, 1041–1048 (2005)
DOI: 10.1051/0004-6361:20053390

Astronomy & Astrophysics

On constructing horizontal branch models

A. Serenelli[1,2] and A. Weiss[1]

[1] Max-Planck-Institut für Astrophysik, Karl-Schwarzschild-Str. 1, 85748 Garching, Germany
e-mail: weiss@mpa-garching.mpg.de
[2] Institute for Advanced Study, Einstein Drive, Princeton, NJ 08540, USA

Received 9 May 2005 / Accepted 28 July 2005

ABSTRACT

We investigate different methods used to construct (zero-age) horizontal branch models and compare the resulting horizontal branch evolution with that of models resulting from the calculation of the complete stellar evolution from the main sequence and through the core helium flash. We show that the approximate methods may lead to small but discernible effects, but that some methods, which are as simple, reproduce the complete evolution very well.

Key words. stars: evolution – stars: horizontal-branch – methods: numerical

1. Introduction

The horizontal branch (HB) in the Hertzsprung-Russell-Diagram (HRD) has a number of important applications. For example, it allows distance-independent age determinations of globular clusters, when the difference between the time-dependent turn-off brightness and the almost time-independent one of the HB is used (e.g., Salaris & Weiss 1997). On the other hand, its brightness or that of RR Lyr stars (Feast 1997) populating it can be used to determine distances. The number of stars on the HB relative to the number of stars on the Red Giant Branch (RGB) above the HB is an indicator for the helium content of the cluster (Buzzoni et al. 1983; Salaris et al. 2004).

Physically, HB stars are in the core helium burning phase following the RGB. The ignition of helium burning takes place under degenerate conditions and is a very energetic and partially dynamic event. Stars of initial mass $M_i \gtrsim 2.3\ M_\odot$ ignite Helium under non-degenerate conditions and populate the equivalent of the HB, the so-called clump, which is observationally a region of increased star density close to or on top of the RGB at the level of the HB.

The distribution of post-flash low-mass stars along a horizontal sequence can be explained by a constant core mass, which is closely related to the luminosity of the star, and a spread in envelope and thus total mass (Faulkner 1966; Dorman 1992). This determines the effective temperature, but only weakly the luminosity. In a globular cluster, due to the fact that all stars have the same age, the initial mass of the stars now populating the HB must have been the same and the spread along the HB must be the result of different mass loss histories.

The detailed distribution of HB stars as function of $T_{\rm eff}$, the so-called HB morphology, appears to be determined primarily by the composition (the "first parameter") and a "second parameter", the nature of which is so far unknown, although age is considered to be a likely candidate (see, for example Lee et al. 1994; Sweigart & Catelan 1998; Catelan 2000). One should add that here secondary age effects are considered, because age itself is a primary parameter, due to the fact that the turn-off mass is already influencing the HB morphology because younger populations, i.e. more massive stars will become more massive, therefore cooler, HB stars.

The evolution to an HB star goes through the violent core helium flash. For several decades, only very few calculations have been able to follow stellar models through this event. The reason is that typical timesteps decrease to the level of seconds because of the rapid change in helium luminosity, which may flare up to $10^{10}\ L_\odot$ for a few days. Because other parts of the star remain completely unchanged during this time, the differencing schemes become numerically unstable and no longer converge. Therefore, full flash calculations were successful in most cases only for higher masses, where degeneracy of the RGB stellar core is lower and the flash milder (see Thomas 1967, for a pioneering study). With a few exceptions, complete stellar evolution tracks into the HB phase were absent.

For this reason most HB models were calculated by starting new sequences on the HB, where the initial structure is taken from that at the tip of the giant branch, and solutions of the structure equations are sought where the effect of the helium flash is taken into account. This implies a reduced core density, hydrostatic helium burning, a lower surface luminosity and an effective temperature depending on the envelope mass. Details of such approximate methods will be given later in the paper. Overall, such starting models represent the true zero-age HB (ZAHB) and the following evolution quite well, but there is no systematic investigation of the effects of the approximation.

The underlying assumption of such methods is that during the helium flash no events take place that modify the internal chemical structure significantly.

Since a few years an increasing number of stellar evolution codes have been improved numerically to a level where full flash calculations have become possible. Still, the computational effort is large, such that grids of HB models derived from complete evolution sequences are not truely practicable. However, it is now possible to compare full with approximate HB models and to design schemes for the construction of HB models which are both economical and accurate. Given the fact that the requirements of accuracy of stellar models is steadily increasing, either from observational data about stars, or – as in the case of the cluster ages – because of more detailed questions to be answered, we must consider the accuracy of HB models.

Recently, Piersanti et al. (2004) published a similar and independent investigation testing their own method for ZAHB model construction. They showed results for two cases, to which we will refer.

In Sect. 2 we will discuss briefly our stellar evolution code and present full core helium flash calculations and the resulting ZAHB models and HB evolution. In Sect. 3 we present several typical schemes to create approximate HB models without following the complete flash. Section 4 is devoted to critically analyzing results for approximate models by using results of Sect. 2 as a reference. We will not investigate methods that rely on a completely new construction of models, since today they are of only historical interest (Rood 1970; Sweigart & Gross 1976). All calculations have been done with the same code to avoid differences resulting from details in the numerical programs. Section 5 provides a short summary.

2. Complete evolution from the ZAMS to the HB

2.1. Code

Throughout this paper we use the Garching stellar evolution code, which has been described in some detail in Weiss & Schlattl (2000). The numerical aspects of this code have been improved such that the evolution of Asymptotic Giant Branch (AGB) stars can be followed through many thermal pulses without convergence problems and intervention (Wagenhuber & Weiss 1994). Due to the same improvements in the algorithms controlling the temporal and spatial discretization the helium core flash also became feasible (Wagenhuber 1996), because the numerical problems encountered in both phases are of a similar nature. It is now possible to calculate through the helium flash even if mixing of protons from the hydrogen layers into the helium burning region occurs, which leads to an additional flash event due to the energy release of carbon conversion to nitrogen. We have presented such calculations both for Pop. III (Schlattl et al. 2001) and Pop. II models (Cassisi et al. 2003). In the latter case, such mixing occurs when the helium flash sets in only after the star has already left the RGB due to high mass loss. For these mixing events, (convective) mixing and nuclear burning of both H and He have to be treated simultaneously because of comparable timescales. In the present paper, such cases will not be considered, because they obviously violate the basic assumption of the approximate models of an unmodified composition profile between the onset of the flash and the ZAHB.

We note that convection is always treated in the most simple way, i.e. using mixing length theory and employing the Schwarzschild criterion for convective stability. We thus consider neither overshooting nor semiconvection. Both effects play a role during the HB evolution, but need additional assumptions and introduce free parameters, which usually are determined from comparison with observations. The inclusion would not change our results significantly, because we are mainly interested in the quality of the constructed ZAHB models.

Table 1. List of models for which we did full evolutions through the helium flash. The columns list metallicity, initial mass, the parameter η in Reimers' mass loss formula, total mass $M_{\rm f}$ after the core helium flash, core mass $M_{\rm c}$, and convective core mass $M_{\rm cc}$ at the ZAHB.

Z	$M/M_\odot$	η	$M_{\rm f}/M_\odot$	$M_{\rm c}/M_\odot$	$M_{\rm cc}/M_\odot$
0.0001	0.80	0.0	0.7971	0.5011	0.131
		0.3	0.6788	0.5014	0.134
		0.5	0.5863	0.5015	0.133
	0.85	0.0	0.8471	0.4996	0.132
		0.5	0.6574	0.4999	0.131
		0.7	0.5632	0.5001	0.132
0.003	0.82	0.0	0.8170	0.4892	0.121
		0.2	0.6650	0.4895	0.121
		0.3	0.5734	0.4897	0.122
	0.90	0.0	0.8970	0.4878	0.121
		0.3	0.6906	0.4879	0.120
		0.5	0.5085	0.4880	0.119

2.2. Calculations

We have evolved low-mass stars between 0.8 and 0.9 $M_\odot$, and compositions of $Z = 0.0001$ and 0.003. The initial helium content was always $Y = 0.25$. A list of cases is given in Table 1. With these parameters we cover turn-off ages between 8 and 12 Gyr years and the lower metallicity range of galactic globular clusters. The evolution was followed from the zero-age main-sequence (ZAMS), starting from a homogeneous model up to the lower AGB, that is, prior to the onset of thermal pulses. For mass loss we used the standard Reimers formula (Reimers 1975),

$$\frac{{\rm d}M}{{\rm d}t} = -4\times10^{-13}\eta\frac{LR}{M}\left(\frac{M_\odot}{L_\odot R_\odot}\right) M_\odot/{\rm yr},$$

varying η between 0.0 (no mass loss) and 0.7 (see Table 1). The two bluest HB models we have computed are those with $Z = 0.003, 0.9\,M_\odot, \eta = 0.5$ and $Z = 0.0001, 0.85\,M_\odot, \eta = 0.7$ which have, on the ZAHB, $T_{\rm eff} = 21\,400$ K and 17 400 K respectively. Our range of parameters resulted from our intention to cover a wide range of final HB configurations. In Fig. 1 we show the evolutionary track of the model with initial and constant mass $M = 0.85\,M_\odot$ and metallicity $Z = 0.0001$ (row 4 of Table 1), which we will use as a typical case in the discussion below.

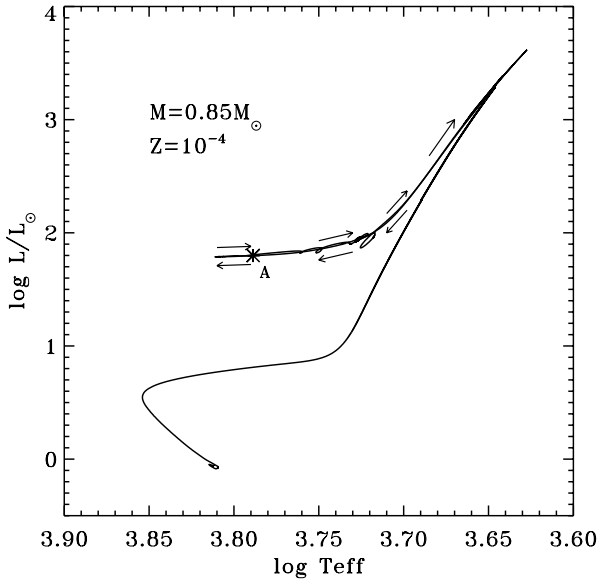

Fig. 1. Global evolution of one of our models from the ZAMS into the early AGB. The sense of evolution from the RGB-tip through the HB and up to the early AGB is indicated by arrows. The location of the ZAHB corresponds to the point labeled *A*. Note that HB evolution is initially bluewards, as shown by the arrows.

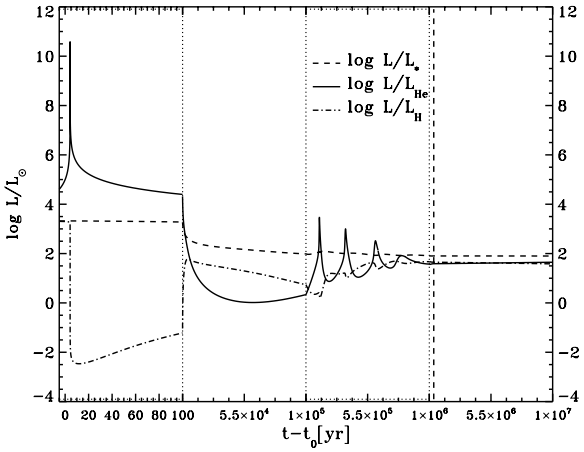

Fig. 2. Evolution of the total, H- and He-burning luminosities for the model shown in Fig. 1 from the onset of the He-core flash until the model has settled on the HB. The moment when the ZAHB is reached is indicated with a vertical dashed line and corresponds to 1.325×10^6 yr after the onset of the flash.

In the calculation of the core helium flash we assume hydrostatic equilibrium. This is certainly not correct, as our tests show. We calculated the acceleration $\partial^2 r/\partial t^2$ of mass shells a posteriori and compared it with the gravitational acceleration. Indeed, the two quantities can become of similar order for a short period after the helium luminosity peak. While our code allows the inclusion of this approximate dynamical term in the hydrostatic equation we have not made use of this feature.

The question of whether the core helium flash is dynamic and whether dynamical episodes are of any consequences for the flash itself and the later evolution is still unclear. Early multi-dimensional calculations by Deupree (Deupree & Cole 1983; Deupree 1984a,b) remained inconclusive, but more recent hydrodynamical calculations (Achatz et al. 2005, in preparation) indicate that the hydrostatic calculations are indeed quite well justified, at least from the point of view of long-term evolution. In the quoted paper neither any loss of envelope mass nor any mixing beyond that predicted by mixing length theory of convection is found. A second argument in favor of the appropriateness of the hydrostatic models is the fact that so far there is no observational indication of unknown effects on the HB, which would point to deviations of the flash evolution from the simple hydrostatic picture. Nevertheless, the issue remains open, but is of no influence for the present investigation, which deals only with the influence of the technical construction of HB models for given physical assumptions.

In Fig. 2 we illustrate the evolution of various quantities of the model of Fig. 1 during the helium flash, demonstrating in particular the extremely short timescales and the amplitude of the helium luminosity $L_{\rm He}$. The evolution during the beginning of the HB is also shown in Fig. 2. While the evolution to the onset of the flash (defined as the moment in which $\log L_{\rm He}/L_\odot = 5$ for the first time) requires about 9000−13 000 timesteps (from the ZAMS) depending on the metallicity and mass of the model, during the flash another 1500 models are needed, with a minimum timestep of about 600 s.

After the core He flash (and a series of small secondary flashes, as can be seen in Fig. 1) convection reaches the center of the star. At that time the central carbon abundance has already risen to $X_{\rm C} = 0.0428$ (from an initial value of 1×10^{-5}) due to the initial 3α-reactions. We define the zero-age on the HB (ZAHB) to be the model in which the integrated thermal energy is smallest. For the case shown this happens 1.325×10^6 years after the onset of the flash (vertical dashed line in Fig. 2 and asterisk in Fig. 1) or, equivalently, 0.4906×10^6 years after convection has reached the center. The central carbon content when the model reaches the ZAHB is $X_{\rm C} = 0.0535$. This value depends only slightly on the mass of the models and on the assumed metallicity (e.g. $X_{\rm C} = 0.05$ for models with $Z = 0.003$). This calculation has been performed without mass loss, therefore resulting in the reddest ZAHB model possible for the chosen mass and composition. In Fig. 3 we display the HB evolution of a number of cases all evolved from the same initial model, but with different mass loss rates during their pre-HB evolution as shown in the diagram (see Table 1). There is no additional or enhanced mass loss during the helium flash except due to changes in the global stellar parameters entering the Reimers' formula. For simplification, we will call HB models obtained from complete evolutionary calculations "full models". Mass loss has been halted after the models reach the ZAHB to facilitate comparison between "full models" and "constructed models" in the following sections.

Stellar evolution during helium-burning phases has been the subject of numerous studies and it is beyond the scope of this article to review this here. One feature, however, is worth commenting on. We find that all of our "full models" undergo, during the transition from helium-core to helium-shell burning phase, a series of small thermal runaways in the helium-shell. These pulses, previously found by Mazzitelli & D'Antona (1986) and Althaus et al. (2002) in the context of the

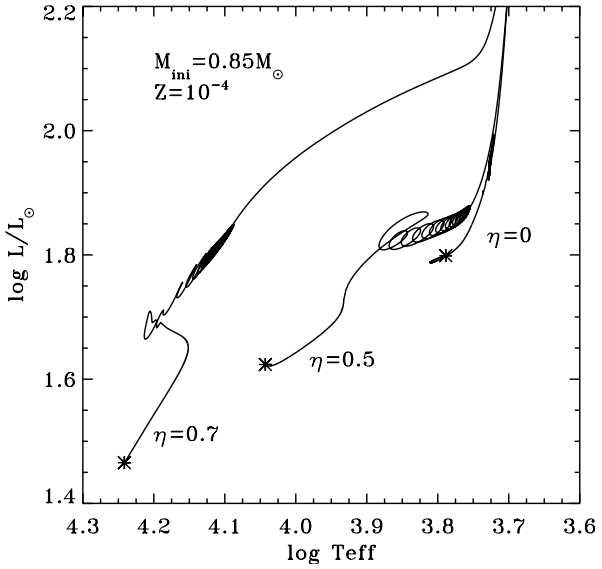

Fig. 3. Horizontal branch evolution for models evolved from the main sequence but with different Reimers mass loss parameter η as indicated in the figure. Initial mass and composition are the same as for the model of Fig. 1. We show only the part starting at the ZAHB, which is indicated by a star.

evolution of a 3 $M_\odot$ stellar model, have been named thermal micropulses because of their resemblance to the thermal pulses of AGB stars. In the HRD, the micropulses are seen as a series of small amplitude loops (see Fig. 3). We find that the occurrence of these pulses is missed, in most cases, if a large enough evolutionary time-step is used in the calculations.

3. Construction methods

In this section we will present a few methods used by research groups working on stellar evolution to construct (ZA)HB models, generally starting from RGB models evolved into the helium flash.

3.1. Method 1: reducing mass along the ZAHB

This method, named M1 hereafter, is our method to construct approximate models and differs from others that we will describe in that it does not start with an RGB, but rather with a ZAHB model obtained from a full evolution without mass loss as in Fig. 1. Once this star settles on the HB and the ZAHB model is identified, the temporal evolution is stopped, and instead mass is removed from the envelope until the total mass desired is reached. The static models obtained after the removal of mass are considered as true ZAHB stars and their evolution on the HB is started without any additional relaxation period. The assumption here is therefore that all ZAHB models originating from the same initial ZAMS model have the same chemical structure *after the flash* independent of their mass loss history. This is confirmed by the full model calculations presented in Sect. 2. In Table 1 the size of the convective core when the models reach the ZAHB is shown to be identical at a level of $10^{-3}\,M_\odot$ irrespective of the mass loss history of the model (it also seems to be quite independent of the initial mass of the model, at least in the range we have studied). The same convergence for different models is observed, as stated previously, in the chemical composition of the core at the ZAHB.

3.2. Method 2: reconfiguration of pre-flash models

This is the standard method for constructing ZAHB models (see Castellani et al. 1989; and Dorman et al. 1991). In this method a model close to or at the beginning of the core helium flash is used as the starting model for the ZAHB construction. The flash itself is not calculated. In particular, the core mass and chemical profile of the pre-flash model are kept constant. The total mass is either preserved, too, or reduced by "rescaling" the envelope (Dorman et al. 1991). The new model on the ZAHB is found by a Runge-Kutta or similar integration with two boundary conditions each at both center and photosphere. The boundary values are initially guessed from known HB structures and modified until the two integrations agree at a predefined fitting point. This new model is then "relaxed" for a certain amount of time or number of timesteps (depending on the implementation) and afterwards identified as the new ZAHB model.

A variant of this method has been used by Sweigart (1987, and private communication 2005) by constructing new ZAHB starting models using homology and other scaling relations and converging these models immediately with the usual Henyey-solver of the stellar evolution code.

From the first calculations (see Sweigart 1987) it was realized that the core composition on the ZAHB will no longer be the one before the flash, because of a modest carbon production during the flash. The initial composition for the new ZAHB model is therefore modified accordingly by hand. The amount of produced carbon added to the core composition varies between 2 and 5% by mass, and can be guided by the simple estimate that the energy needed for the expansion of the degenerate helium core must come from helium burning (Iben & Rood 1970). In the present study, for which we have full models available, we generally used a value of 5% in our calculations, following the results of the calculations presented in Sect. 2. We also tested 2% and 3% to investigate the importance of this guess.

Piersanti et al. (2004) investigated the accuracy of "pseudo-evolutionary" ZAHB models generated in that way. The relaxation period for these models is 1 Myr to allow adjustment of CNO equilibrium to the new thermal structure in the shell region; the additional carbon abundance is 5%. In that paper comparisons with full models are shown and discussed briefly for $M = 0.9$ and $0.794\,M_\odot$ ($Z = 0.0001$; $Y = 0.23$). The latter case is comparable to our first one of Table 1. Note that the core mass in our case is $M_c = 0.5011\,M_\odot$, while it is $0.5185\,M_\odot$ in that of Piersanti et al. (2004). This reflects the different initial helium content as well as differences in the treatment of physical aspects like neutrino cooling or electron conduction.

The details of our implementation of this method are as follows. We evolve RGB models until the onset of the flash ($\log L_{\rm He}/L_\odot = 5$). We then keep total mass and chemical profile (i.e. the values of core and envelope mass) fixed, construct

a static HB model using the Runge-Kutta integrator, which is an integral part of our stellar evolution code and then add 5% of carbon to the homogeneous helium core. In the full models, the time between the onset of the He-flash and the model reaching the ZAHB is $\sim 1.3 \times 10^6$ years (a value which depends little on the metallicity and mass of the model) and during this time some hydrogen burning in the shell also occurs (^{12}C is transformed to ^{14}N in the layers surrounding the H-burning shell as they get hotter during the contraction phase from the tip of the RGB to the HB). To account for this effect, we let the model relax the CNO elements in the H-shell of the initial HB model for 1.5 Myr while keeping the He content of the core fixed (it is not a crucial point whether relaxation is allowed for 1.5 or 1.3 Myr because in both cases CNO abundances rearrange conveniently; note that also the consumption of protons is taken into account). The resulting model is assumed to be the new ZAHB model. In method M1 this is not necessary, because the method relies on a full model. To minimize the number of necessary assumptions when using this method we have not applied any envelope rescaling, i.e. for each HB model we have evolved accordingly a model from the ZAMS to the RGB-tip with the appropriate mass loss rate and then relaxed it with the Runge-Kutta integrator. We call this method M2.

3.3. Method 3: rescaling a single initial model

This method (M3) is a derivation of the method M2 presented in the previous section. First, an HB model corresponding to a stellar model evolved from the ZAMS without mass loss is constructed with method M2 and the ZAHB model is identified. This gives the reddest possible ZAHB corresponding to a given ZAMS model. A sequence of ZAHB models with smaller envelopes can now be constructed by removing mass from the envelope until the desired total mass is reached (in this point it resembles method M1). Numerically, it represents a simplification with respect to methods M1 and M2. In the first case, because no full flash calculation is needed, and in the second case because only one RGB evolution is needed and it is usually easier to remove mass than to relax an RGB model with a Runge-Kutta integrator.

3.4. Method 4: relaxing a step-like chemical profile

One further simplification that can be done to generate HB models, which is equivalent to creating them from scratch, is to avoid the calculation of an RGB model at all. This can be easily done by assuming a total and a core mass for the model, and giving the desired composition for the core and the envelope assuming a step-like shape at the core mass. Because the required input information for a Runge-Kutta relaxation is the chemical profile and the boundary conditions, HB models can be generated in this way without involving the calculation of any previous stage of the evolution of the models. Once the initial HB models are computed, CNO abundances are relaxed as described in Sect. 3.2. This is method M4.

4. Results and discussion

We now compare the HB models constructed with the approximate methods described in the previous section with the full models presented in Sect. 2. We find that the results of comparing approximate models to full models can be classified in terms of the location of the models on the HB, i.e. in terms of their effective temperature. This is related to the morphology of the evolutionary track on the HB which, as can be seen in Fig. 2, depends on the effective temperature of the models. In this way, we group our models into cool ($\log T_{\rm eff} \leq 3.85$), intermediate ($3.85 \leq \log T_{\rm eff} \leq 4.10$) and hot models ($\log T_{\rm eff} \geq 4.1$) and discuss our results in terms of this classification.

We have employed method M4 to construct models corresponding to the $M = 0.80\,M_\odot$, $\eta = 0.3$ and $M = 0.82\,M_\odot$, $\eta = 0.2$ full models. The difference in effective temperature and luminosity between the models constructed with this method and full models is approximately 5% along the whole HB evolution. This level of agreement, although reasonably good considering that the models are basically constructed from scratch, is at least a factor of two worse than that obtained with any of the other methods presented in this paper as will be shown below. For this reason, no further tests have been carried out with method M4. We focus our discussion on methods M1, M2 and M3, which have been used to obtain HB models for all relevant cases presented in Table 1.

In Fig. 4 we present the results for a typical *cool* HB model ($Z = 0.003$, $M = 0.6906\,M_\odot$). The top panel shows the evolution of the model in the HRD. Results for the M1, M2 and M3 methods are also shown but are almost indistinguishable in this plot. Differences in luminosity and effective temperature with respect to the full model as a function of time are also displayed in the plot. The two panels of the central plot show the behavior of luminosity against time during HB evolution for the full and M1, M2, and M3 models, and the relative difference in luminosity for the approximate models with respect to the full one. All methods give good agreement with predictions of the full model for most of the HB evolution and curves overlap in the luminosity plot. However, it can be seen that in the last stages of the HB evolution (between 35 and 45 Myr), M2 and M3 models deviate from the full model, with differences that reach up to 4% for M3 model and more than 5% in the case of method M2. The reason for the difference is that for the M2 model, evolution is slightly slower than in the full model, while for M3 the situation is reversed. Deviations are more noticeable at the last stages of HB evolution because at those stages luminosity changes occur on much shorter timescales than in previous stages. The M1 model completely overlaps the full model in luminosity plot and this can also be seen as a constant difference of about 0.5% with respect to the full model during the whole HB evolution. The bottom panels show the behavior of effective temperature against time in the same fashion as for luminosity. The conclusions are qualitatively the same. The relative differences between M2 and M3 with respect to the full model are much smaller in magnitude and the sign is the opposite to that of the luminosity differences. Again, method M1 yields the most accurate agreement with the full models. Although all full and approximate models move

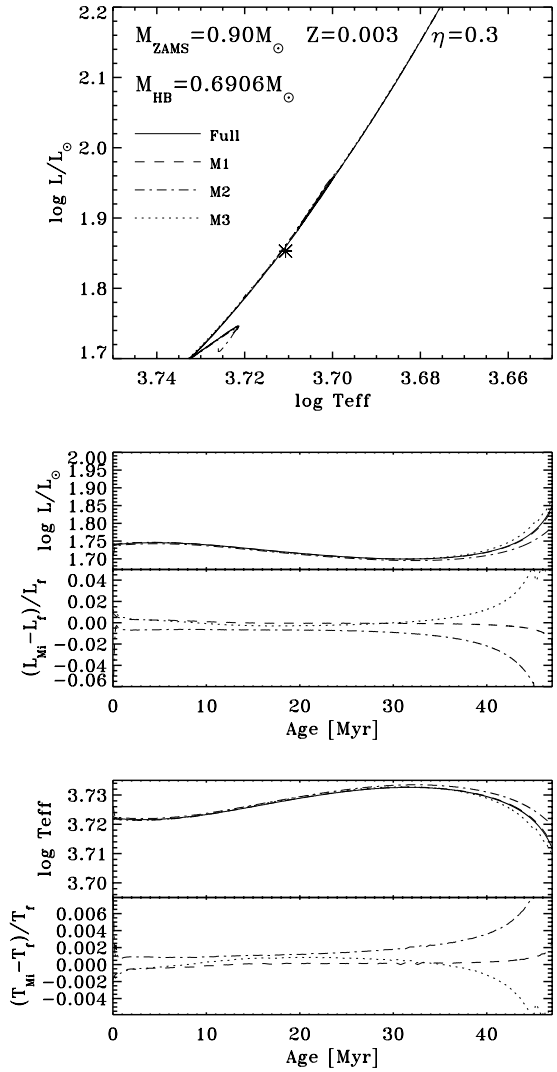

Fig. 4. Comparison between full and approximate models constructed with methods M1, M2 and M3 for a typical cool (red) HB stellar model. *Top panel*: evolution in the HRD, starting with the ZAHB and up to the early AGB. The characteristics of the progenitor and the mass of the model on the HB are indicated, as well as the meaning of the different linetypes. The asterisk denotes the point where the central helium mass fraction drops below 0.01 in the full model (in the scale of this plot, however, equivalent points in all sequences overlap almost completely). *Middle panels*: luminosity and relative luminosity differences for approximate models with respect to the full model against time. Indices f and Mi indicate full models respectively the i-th method. *Bottom panels*: effective temperature and relative effective temperature differences against time. Ages are counted from the ZAHB. Middle and lower panels show the evolution until the end of the HB evolution only, defined by the end of core helium burning.

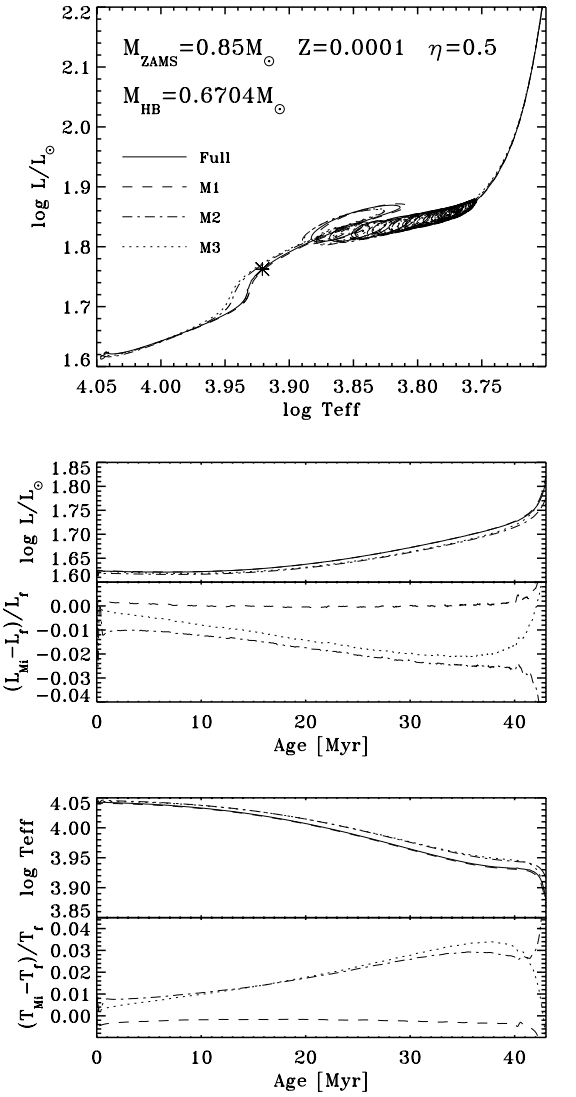

Fig. 5. The same as Fig. 4 but for a typical intermediate HB model. Characteristics of the model are given in the top panel.

along the same evolutionary track as seen in the HRD, they do it at somewhat different speeds so that at a given age they are in slightly different positions on it. This may have some influence on applications based on star counting on the HB, although the effect will be rather small, since the age differences generally remain below 1 Myr.

We discuss now our results for *intermediate* HB models, i.e. those with effective temperatures around 10 000 K. As a representative of this group we show the model with $Z = 0.0001$ and $M = 0.6704\,M_\odot$, as indicated in the top panel of Fig. 5, where the HRD evolution of the full and approximate models are also presented. In this case, the HRD diagram reveals some differences between the full and corresponding M2 and M3 models, especially noticeable at about $\log T_{\rm eff} \approx 3.94$. The M1 model, on the other hand, completely overlaps the full model for the whole HB evolution (which ends at the point marked with an asterisk). In the middle and bottom panels it is clearly seen that the M1 model also gives a very good agreement with the full model for the temporal evolution of luminosity and effective temperature (at the level of 0.4% or less). M2 and M3 models have very similar behavior, where the deviations with respect to the full model increase monotonically during almost all the HB evolution and reach values that vary between 2 and 4%.

The case for a *hot* HB model is presented in Fig. 6, where results for the model $Z = 0.0001$ and $M = 0.5863\,M_\odot$ are shown. Model M1 performs very well in this case, too, at the

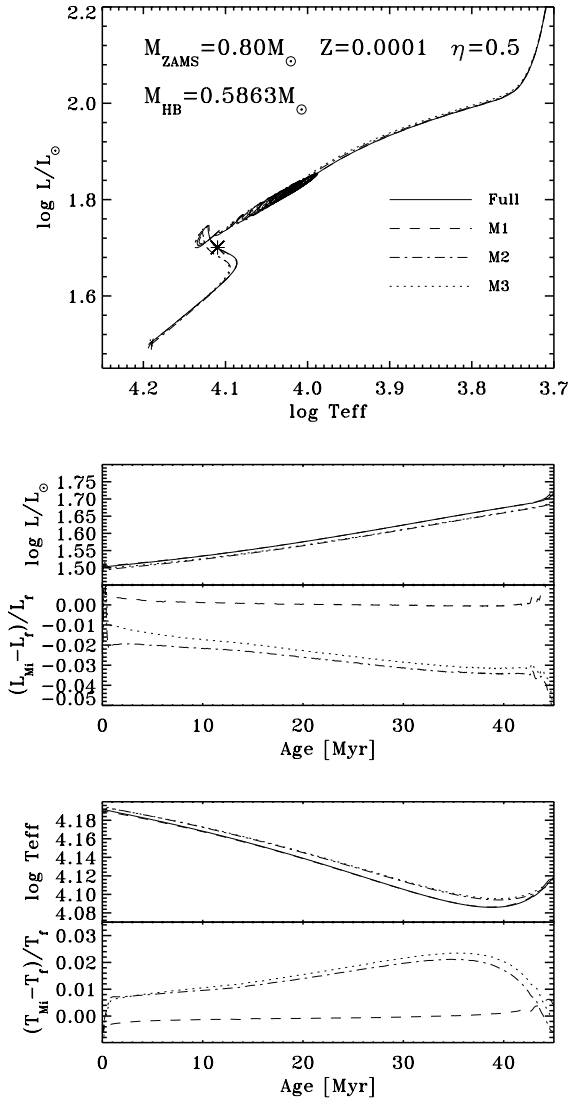

Fig. 6. The same as Fig. 4 but for a typical hot HB model. Characteristics of the model are given in the top panel.

same level as in the preceding cases. It cannot be distinguished from the full model in the HRD and in the plots where luminosity and effective temperature are given as a function of time. Models constructed with methods M2 and M3 lead to a slightly different HRD evolution than the full or M1 models. Also, as in the case for intermediate HB models, the difference between these models and the full model tends to increase with time. Notice that the lower panels only cover the evolution up to the end of the HB; after that, during the micropulses, the deviations become much larger because of the rapid changes in luminosity and effective temperature (Fig. 6, upper panel). On average, however, good agreement is still present.

The most extreme HB model we have calculated ($Z = 0.003$, $0.9\,M_\odot$, $\eta = 0.5$) has $\log T_{\rm eff} \approx 4.32$. The location on the HRD of such extreme models, for a given stellar mass, is extremely dependent on the hydrogen-depleted core mass (or, for a given core mass, on the envelope mass). The full model has total mass $M_{\rm HB} = 0.5085\,M_\odot$ and core mass $M_{\rm c} = 0.4880\,M_\odot$. The corresponding M1 model, constructed from the $Z = 0.003$, $0.9\,M_\odot$, $\eta = 0$ model has the same total mass by construction but its hydrogen-depleted core mass is $M_{\rm c} = 0.4878\,M_\odot$. This very small (0.04%) difference in the core size translates into 1% in the envelope mass. As a result, the M1 model effective temperature and luminosity along the HB differ by about 1% and 0.5% from those of the full model respectively.

There is another complication for even higher mass loss and thus even more extreme HB models. Above the hydrogen burning shell there is always a region of varying CNO-abundances (mostly C and O are reduced) due to partial CNO-cycling. With increasing mass loss on the RGB this region is squeezed closer to the shell. However, even for method M1, our approach rests on the assumption that the chemical profile is independent of the mass loss history, which in this extreme case, is no longer justified. In practice, if we were to construct ZAHB models with total mass of order $0.55\,M_\odot$ or below, we would remove part of the region of varying composition, uncovering processed layers, in contrast to full models. While there might not be a significant change in the following HB evolution, the surface composition will be incorrect. We have therefore avoided such extreme models and recommend full models in such cases. Sweigart (2005, private communication) has been using a method similar to M1 which considers the abovementioned effect as well by reducing the mass of the C- and O-depleted regions.

Methods M2 and M3 provide the freedom of choosing the central composition of the ZAHB model, i.e. how much helium is assumed to have been converted into carbon during the flash. Based on full calculations, our standard choice for M2 and M3 models has been that 5% of the mass in the core is carbon at the ZAHB. We have tried, however, some models where this value was set to 2 and 3%. The first choice does not give a good agreement with full models. If 3% of carbon in the core is assumed, then the quantitative agreement with full models is similar to that of M2 and M3 models with 5% initial carbon content, the discrepancies being of opposite signs. This seems to suggest that 4% of the central carbon abundance is the best choice for M2 and M3 methods, a value that is, however, not the one indicated by full models and implies that M2 and M3 models may require fine tuning to reproduce results as good as those of the M1 method.

Finally, we have computed a few cases where full models were computed including microscopic diffusion from the ZAMS. We have tested our M1 method against these models and found the same performance as described above for models without diffusion. This is an expected result, basically because method M1 incorporates, by construction, all the hypotheses used in the computation of the full model from which M1 models are constructed.

5. Summary and conclusions

The aim of the paper is to analyze the accuracy of HB models constructed with a variety of approximate methods by comparing them to full evolutionary models, i.e. models obtained by following their evolution from the ZAMS up to the RGB-tip and through the core helium flash. In particular, we present our method (M1) which consists of evolving a given initial ZAMS model without mass loss all the way from the ZAMS to the

ZAHB and then removing envelope mass while stopping the evolution to get the final HB model mass desired. In this way, a whole HB sequence can be built with a negligible amount of effort once the first ZAHB model is given. Other, and maybe more important, advantages of this method are that no guess for the amount of helium burned during the flash and no relaxation time to adjust CNO abundances in the hydrogen shell are needed. These last two points are potential sources of uncertainties in the methods usually presented in the literature (see description of methods M2 and M3 in Sect. 3). Comparison with the full models shows that any of the three methods discussed in this paper give reliable HB models, but the performance of method M1 is outstanding. This is, then, our preferred method.

We confirm the results by Piersanti et al. (2004) about their method (M2), but find that this and method M3 are less accurate in particular for hotter HB stars. With increasing $T_{\rm eff}$ (decreasing envelope mass) the discrepancies are at a level of a few per cent. Also, details of the post-HB evolution (micropulses) differ. However, this phase also depends on the treatment of convection on the HB, such that we did not consider these events in detail.

While we have not investigated cases with overshooting or some treatments of semiconvection, our results are unlikely to change, in particular because the FRANEC code used in Piersanti et al. (2004) incorporates the latter and our results agree with theirs.

Acknowledgements. We thank S. Degl'Innocenti, L. Girardi, and S. Cassisi for information concerning their methods for constructing horizontal branch models. H. Schlattl supported us in the calculations of full flash models and had the original idea for our prefered method M1. We thank in particular A. Sweigart for an excellent referee report which contained very valuable additional information and helped to improve this paper.

AMS has been supported in part by the European Association for Research in Astronomy through its EARASTARGAL program, the W. M. Keck Foundation through a grant to the Institute for Advanced Study and the NSF through the grant PHY-0070928. We are grateful for the hospitality we experienced at our visits at MPA (Garching) and IAS (Princeton).

References

Althaus, L. G., Serenelli, A. M., Córsico, A. H., & Benvenuto, O. G. 2002, MNRAS, 330, 685
Buzzoni, A., Pecci, F. F., Buonanno, R., & Corsi, C. E. 1983, A&A, 128, 94
Cassisi, S., Schlattl, H., Salaris, M., & Weiss, A. 2003, ApJ, 582, L43
Castellani, V., Chieffi, A., & Pulone, L. 1989, ApJ, 344, 239
Catelan, M. 2000, ApJ, 531, 826
Deupree, R. G. 1984a, ApJ, 282, 274
Deupree, R. G. 1984b, ApJ, 287, 268
Deupree, R. G., & Cole, P. W. 1983, ApJ, 269, 676
Dorman, B. 1992, ApJS, 80, 701
Dorman, B., Lee, Y., & Vandenberg, D. A. 1991, ApJ, 366, 115
Faulkner, J. 1966, ApJ, 144, 978
Feast, M. W. 1997, MNRAS, 284, 761
Iben, I. J., & Rood, R. T. 1970, ApJ, 161, 587
Lee, Y., Demarque, P., & Zinn, R. 1994, ApJ, 423, 248
Mazzitelli, I., & D'Antona, F. 1986, ApJ, 308, 706
Piersanti, L., Tornambè, A., & Castellani, V. 2004, MNRAS, 353, 243
Reimers, D. 1975, Mem. Soc. Roy. Sci. Liège, 8, 369
Rood, R. T. 1970, ApJ, 161, 145
Salaris, M., Riello, M., Cassisi, S., & Piotto, G. 2004, A&A, 420, 911
Salaris, M., & Weiss, A. 1997, A&A, 327, 107
Schlattl, H., Cassisi, S., Salaris, M., & Weiss, A. 2001, ApJ, 559, 1082
Sweigart, A. V. 1987, ApJS, 65, 95
Sweigart, A. V., & Catelan, M. 1998, ApJ, 501, L63
Sweigart, A. V., & Gross, P. G. 1976, ApJS, 32, 367
Thomas, H.-C. 1967, Z. Astrophys., 67, 420
Wagenhuber, J. 1996, Ph.D. Thesis, Techn. Univ. München
Wagenhuber, J., & Weiss, A. 1994, A&A, 286, 121
Weiss, A., & Schlattl, H. 2000, A&AS, 144, 487